

ESTABLISHING A NON-CRITICAL BASELINE FOR FLUCTUATION OBSERVABLES*

ANAR RUSTAMOV

GSI Helmholtzzentrum für Schwerionenforschung, Darmstadt, Germany
and
National Nuclear Research Center, Baku, Azerbaijan

(Received December 15, 2020)

Non-critical contributions are discussed in the context of fluctuations of conserved charges, which are of particular importance for disentangling critical signals originating from second order phase transitions. The approach is based on a model-independent construction of canonical partition function, *i.e.*, by using measured mean multiplicities of baryons and anti-baryons. The experimental measurements of the STAR and ALICE collaborations are confronted with the presented model predictions. For this purpose, in line with the experimental observations, different acceptances are introduced for baryons and anti-baryons. It is demonstrated that nearly all measured experimental signals of net-proton cumulants, up to order four, can be described by accounting for global baryon number conservation. A dedicated Python package is developed in order to obtain analytical expressions for cumulants of any order of net-baryon (net-proton) distributions. Moreover, it is demonstrated that contributions due to local baryon number conservation at the LHC energies are negligible, which implies sensitivity of measured second order cumulants to early stages of collisions.

DOI:10.5506/APhysPolBSupp.14.353

1. Introduction

Unraveling the phase structure of Quantum Chromodynamics (QCD) is one of the goals of current experimental and theoretical studies of nuclear interactions [1–3]. As QCD, the gauge field theory of strong interaction, has specific features, asymptotic freedom and confinement, in the realm of high temperature and/or density, the fundamental degrees of freedom of the strong interactions come into play [1]. By colliding heavy ions at different

* Presented at the on-line meeting on *Criticality in QCD and the Hadron Resonance Gas*, Wrocław, Poland, 29–31 July 2020.

energies, one hopes to heat and/or compress the matter to energy densities at which a transition from matter consisting of confined baryons and mesons to a state of liberated quarks and gluons (deconfined phase) begins. However, liberated quarks and gluons are not what one ultimately observes in experiments. The subsequent expansion and cooling of the deconfined phase leads to formations of hadrons, which fly outwards, and get registered by the detectors. This process of hadronization plays a key role in understanding what detectors see. The headway is to establish a bridge between the events which occur before the hadronization and the experimental outcome. The situation is much similar to reconstruction of the cosmological Big Bang from observables such as Hubble expansion, the cosmic microwave background and the abundance of light atomic nuclei.

At finite quark masses, the chiral $SU(2)_L \times SU(2)_R$ symmetry is explicitly broken in the QCD vacuum. Moreover, it is well-established through lattice QCD (LQCD) investigations [4] that chiral symmetry is restored in a crossover transition at vanishing net-baryon density and a (pseudo-critical) temperature of $T_{pc} \simeq 156.5$ MeV [5]. The latter is in agreement with the chemical freeze-out temperature as extracted by comparing Hadron Resonance Gas (HRG) model predictions [2] to the hadron multiplicities measured by ALICE. This agreement implies that strongly interacting matter, created in collisions of Pb nuclei at the LHC energies, freezes out in close vicinity of the chiral phase transition line. Hence, singularities stemming from the proximity to genuine second order chiral phase transition, which belongs to the $O(4)$ universality class [6] in the limit of massless u and d quarks, can be captured experimentally in high-energy nuclear collisions, such as those performed at the LHC and top RHIC energies.

At present, systematic LQCD studies of the properties of QCD matter are possible only at small net-baryon densities. Consequently, first-principle results on the nature of the chiral transition at high baryon densities are not yet available. However, studies of strongly interacting matter in effective models of QCD suggest that, at sufficiently large baryon chemical potential μ_B , QCD matter exhibits a first order chiral phase transition [7–15].

The endpoint of such a first-order transition line in the (T, μ_B) -plane is the conjectured chiral critical endpoint (CP) [7]. At such a CP, the system would exhibit a 2nd order phase transition belonging to the $Z(2)$ universality class.

Phase transitions are usually studied by looking to the response of the system to external perturbations. For example, the liquid gas phase transition can be probed by the response of the volume to a change in pressure, which is encoded in the isothermal compressibility. In the Grand Canonical Ensemble (GCE) formulation of statistical mechanics the latter contains fluctuations of liquid constituents from from one microstate to another one.

Hence, the objective is to relate macroscopic parameters of the system, which define its EoS, with its microscopic details encoded in fluctuations. In a similar way, phase transitions in strongly interacting matter can be addressed by investigating the response of the system to external perturbations via measurements of fluctuations of conserved charges such as baryon number or electric charge [16, 17].

Important research objectives are pursued by the ALICE Collaboration at the LHC [18–20], the STAR Collaboration at RHIC [21], the NA61 Collaboration at the CERN SPS [22], and by the HADES Collaboration at the GSI [23].

In order to draw firm conclusions about the structure of the QCD phase diagram, further in-depth studies of all mechanisms leading to deviations from the HRG baseline should be considered [24–30]. In the following, a robust non-critical baseline is presented, which is relevant for the interpretation of experimental results on event-by-event fluctuations of the net-baryon number in nuclear collisions.

2. Correlations induced by baryon number conservation

In a thermal system with an ideal gas EoS, composed of baryon/anti-baryon species with baryon numbers $+1$ and -1 , GCE partition function yields the uncorrelated Poisson distributions for baryons and anti-baryons, hence the net-baryon distribution has the following cumulants [27]¹:

$$\kappa_n(\text{Skellam}) = \langle n_B \rangle + (-1)^n \langle n_{\bar{B}} \rangle, \quad (1)$$

where $\langle n_B \rangle$ and $\langle n_{\bar{B}} \rangle$ denote the first cumulants (mean numbers) of baryons and anti-baryons, respectively. Equation (1) implies that ratios of even-to-even and odd-to-odd cumulants of net-baryons are always unity, while the ratios of odd-to-even cumulants depend on mean multiplicities

$$\frac{\kappa_{2n+1}}{\kappa_{2k}} = \frac{\langle n_B \rangle - \langle n_{\bar{B}} \rangle}{\langle n_B \rangle + \langle n_{\bar{B}} \rangle}. \quad (2)$$

Hitherto, the above conditions are used as a baseline for net-baryon fluctuations. However, this can lead to misleading conclusions because, apart from dynamical fluctuations induced by critical phenomena, deviations from this baseline may be driven by event-by-event baryon number conservation. In order to quantify such non-dynamical deviations from the GCE baseline, the following canonical partition function for a system of baryons/anti-baryons in a finite volume V and temperature T is considered [31–33]:

¹ The probability distribution of the difference of two random variables each generated from uncorrelated Poisson distributions is called the Skellam distribution.

$$\begin{aligned}
Z_B(V, T) &= \sum_{N_B=0}^{\infty} \sum_{N_{\bar{B}}=0}^{\infty} \frac{(\lambda_B z_B)^{N_B}}{N_B!} \frac{(\lambda_{\bar{B}} z_{\bar{B}})^{N_{\bar{B}}}}{N_{\bar{B}}!} \delta(N_B - N_{\bar{B}} - B) \\
&= \int_0^{2\pi} \frac{d\phi}{2\pi} e^{-iB\phi} \exp\left(\lambda_B z_B e^{i\phi} + \lambda_{\bar{B}} z_{\bar{B}} e^{-i\phi}\right) \\
&= \left(\frac{\lambda_B z_B}{\lambda_{\bar{B}} z_{\bar{B}}}\right)^{\frac{B}{2}} I_B\left(2z\sqrt{\lambda_B \lambda_{\bar{B}}}\right), \tag{3}
\end{aligned}$$

where I_B denotes the modified Bessel function of the first kind and $z = \sqrt{z_B z_{\bar{B}}}$. The single particle partition functions for baryons z_B and anti-baryons $z_{\bar{B}}$ involve integrations over position and momentum space, and are directly related to the mean number of baryons and anti-baryons in the grand canonical ensemble $\langle N_B \rangle_{\text{GC}} = e^{\mu_B/T} z_B$ and $\langle N_{\bar{B}} \rangle_{\text{GC}} = e^{-\mu_B/T} z_{\bar{B}}$. It follows that $z = \sqrt{\langle N_B \rangle_{\text{GC}} \langle N_{\bar{B}} \rangle_{\text{GC}}}$.

The auxiliary parameters $\lambda_{B, \bar{B}}$ are introduced for the calculation of the mean number of baryons and anti-baryons. In the final results, they are set equal to unity. The resulting mean multiplicities in the canonical ensemble are²

$$\langle N_B \rangle = \lambda_B \left. \frac{\partial \ln Z_B}{\partial \lambda_B} \right|_{\lambda_B, \lambda_{\bar{B}}=1} = z \frac{I_{B-1}(2z)}{I_B(2z)}, \tag{4}$$

$$\langle N_{\bar{B}} \rangle = \lambda_{\bar{B}} \left. \frac{\partial \ln Z_B}{\partial \lambda_{\bar{B}}} \right|_{\lambda_B, \lambda_{\bar{B}}=1} = z \frac{I_{B+1}(2z)}{I_B(2z)}. \tag{5}$$

From Eq. (3) it follows that, for a given value of net-baryon number B of the full system, the underlying normalized canonical probability distribution for $N_{\bar{B}}$ is given by

$$P_B(N_{\bar{B}}) = \frac{1}{I_B(2z)} \frac{z^B z^{2N_{\bar{B}}}}{(N_{\bar{B}} + B)! N_{\bar{B}}!}. \tag{6}$$

Equation (6) is used to generate the number of anti-baryons $N_{\bar{B}}$ and baryons $N_B = N_{\bar{B}} + B$ in full phase space.

The local baryon number conservation is introduced by exploiting an additional parameter Δy_{corr} , which regulates the strength of the correlation between baryons and anti-baryons in the rapidity space [27]

$$|y_{\bar{B}} - y_B| < \frac{\Delta y_{\text{corr}}}{2}, \tag{7}$$

² Expectation values without a subscript, $\langle \dots \rangle$, refer to the canonical ensemble (3).

where, y_B and $y_{\bar{B}}$ stand for baryon and anti-baryon rapidity values generated from experimentally measured dn/dy distributions. In this picture, the global baryon number conservation corresponds to $\Delta y_{\text{corr}} = 2 \times y_{\text{beam}}$.

3. Experimental results and model predictions

Figure 1 presents the energy dependence of the normalized cumulants. The Canonical Ensemble (CE) baselines, both analytical calculations (red squares or solid red lines) and generated values (solid blue circles) are computed at four different collision energies of $\sqrt{s_{NN}} = 8.8, 17.3, 27$ and 62.4 GeV. For each collision energy, using experimentally measured/estima-

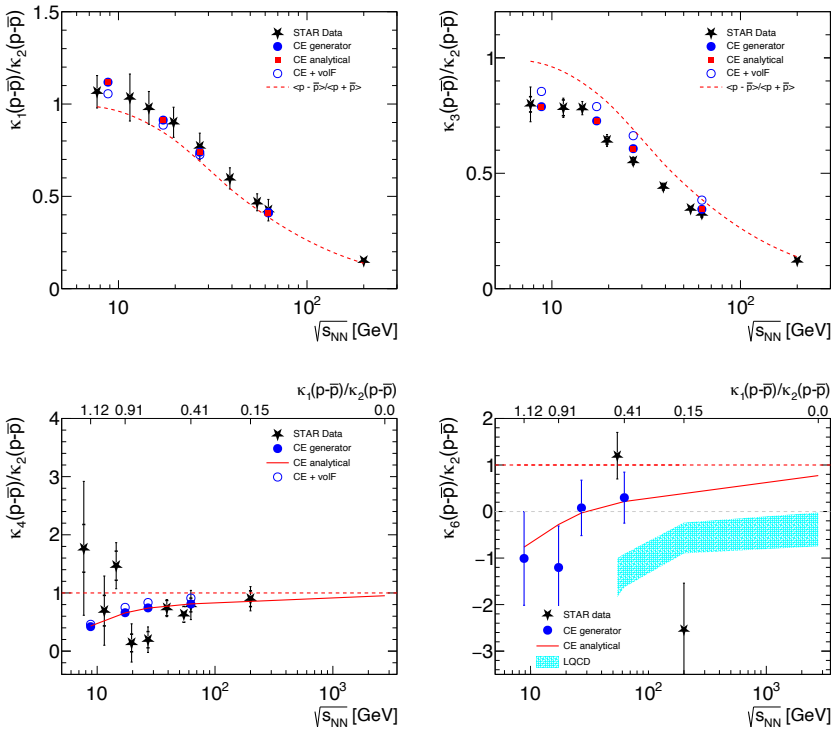


Fig. 1. (Colour on-line) Cumulant ratios of the net-proton distributions. The dashed/red line shows the HRG value [2]. The blue circles show the results of the simulation, while the red squares and solid lines indicate those of the analytical calculations. In both, baryon number conservation is accounted for. They should be compared to the black stars representing experimental results of the STAR Collaboration [21]. Open blue circles include the additional contributions from reaction volume fluctuations [24]. Also shown as the grey/cyan band in the lower right figure is the result from LQCD [34].

ted number of baryons in 4π , Eq. (4) is solved for single particle partition z [3]³. Next, the finite acceptance is introduced by using the measured/predicted rapidity distributions of baryons/anti-baryons from the NA49 [35] and BRAHMS [36] experiments. In addition, the p_T coverage and other contributions, such as those originating from weakly decaying hadrons *etc.*, are introduced by using mean multiplicities of protons and anti-protons as measured by the STAR experiment. Thus all presented model results are computed within the STAR acceptance for cumulant analyses, delimited as $|y| < 0.5$ and $0.4 < p_T < 2$ GeV/ c , independent of collision energy. The corresponding analytical formulas given in Ref. [3] can also be obtained by using the dedicated Python package [37]. For the generated values, the probability function is used as defined in Eq. (6). Also shown for reference is the HRG line denoting the baseline for independent Poissonian fluctuations of protons and anti-protons, *cf.* Eq. (1). For κ_1/κ_2 and κ_3/κ_2 , this corresponds to $\langle n_p - n_{\bar{p}} \rangle / \langle n_p + n_{\bar{p}} \rangle$, while for the ratio of even cumulants such as κ_4/κ_2 and κ_6/κ_2 , it is equal to unity. In general, there is good agreement over the full energy range covered experimentally between the CE baseline (baryon number conservation) and the STAR data. For κ_1/κ_2 , the effect of baryon number conservation is small in the energy range shown here and the canonical baselines are in excellent agreement with the STAR data. Within the experimental uncertainties, the corresponding HRG baseline for the ratio κ_1/κ_2 is also in marginal agreement with the STAR data. For all cumulant ratios the STAR data, as the canonical baseline, approach the HRG limit for higher energies. This behaviour is a consequence of the decreasing acceptances for protons and anti-protons, see the text above. Indeed, a fixed acceptance in rapidity, independent of the collision energy, effectively leads to a decreasing fraction of accepted protons with increasing energy, thereby reducing the effect of baryon number conservation. For the κ_3/κ_2 ratio, the CE baseline is systematically below the corresponding HRG reference. Moreover, this amount of suppression is consistent with the measured STAR data. The κ_4/κ_2 results from STAR exhibit statistical fluctuations around the CE baseline. The Kolmogorov–Smirnov test shows that there is no statistically significant deviation between the CE baseline and the STAR data [3]. In conclusion, within the uncertainties, the energy dependence of cumulants up to order four, measured by the STAR experiment, can be explained with the global baryon number conservation. The situation is different for the κ_6/κ_2 ratio, the CE baseline indicates significant suppression, with respect to unity (HRG line), and even becomes negative at low energies. While at $\sqrt{s_{NN}} = 54.4$ GeV, the STAR data point has positive value and is consistent with the HRG and CE baselines, at 200 GeV the data is

³ At $\sqrt{s_{NN}} = 27$ GeV, model calculations are performed differently, see for details Ref. [3].

significantly below the CE baseline. Moreover, this observation by STAR is not consistent with the presented LQCD results, where the κ_6/κ_2 values, at both collision energies, remain negative [34].

In Fig. 2, the acceptance dependence of the normalized second cumulants of net-protons $R_1 = \kappa_2/\langle n_p + n_{\bar{p}} \rangle$, measured by the ALICE Collaboration in Pb–Pb collisions at $\sqrt{s_{NN}} = 2.76$ TeV, are presented [18, 20]. The analysis is performed with the Identity Method [38–42] in eight pseudorapidity regions ranging from $-0.1 < \eta < 0.1$ up to $-0.8 < \eta < 0.8$. The data exhibits linear approach to unity with decreasing acceptance, consistent with predictions based on the assumption of global baryon number conservation, depicted as the black/pink band [3, 24]. When imposing a finite acceptance cut, the subtle correlations between baryons and anti-baryons, induced by the global baryon number conservation law, weakens. In the limit of small acceptance, these correlations become not visible anymore in the measured second order cumulants. However, the amount of correlation inside finite acceptance depends also on the correlation length Δy_{corr} in the rapidity space (*cf.* Eq. (7)). This local baryon number conservation [27] would lead to further suppression of the measured R_1 values. Close inspection of Fig. 2, however, indicates that within experimental uncertainties, the ALICE data are best described with the large correlation length in the rapidity space, *i.e.*, the observed

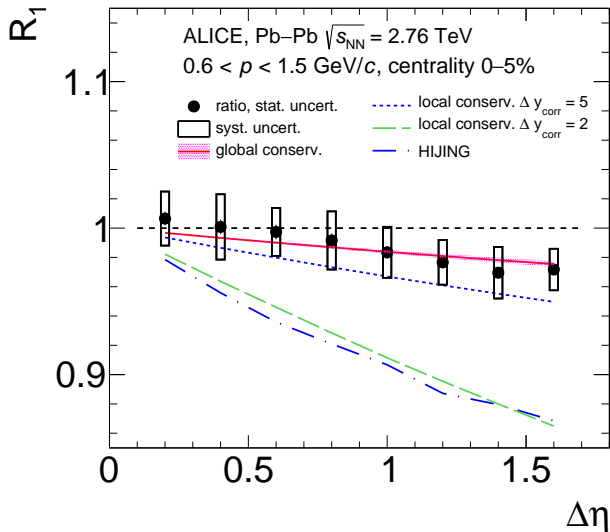


Fig. 2. (Colour on-line) Pseudorapidity dependence of the normalized second cumulants of net-protons $R_1 = \kappa_2/\langle n_p + n_{\bar{p}} \rangle$. Global baryon number conservation is depicted as the black/pink band [3, 24]. The dashed lines represent the predictions from the model with local baryon number conservation [27]. The blue dash-dotted line, represents the prediction using the HIJING generator.

correlations, to a large extent, are induced by global baryon number conservation. The HIJING results [43], on the other hand, underestimate the experimental data and correspond to correlation length of $\Delta y_{\text{corr}} = 2$. The large correlation length observed in the data implies that the normalized second cumulant R_1 is determined by collisions in the very early phase of the Pb–Pb interaction [44].

4. Conclusions

The non-critical canonical baseline is presented for net-baryon cumulants in relativistic nuclear collisions. The net-baryon cumulants are evaluated analytically in the framework of the canonical formulation of statistical mechanics, in which the single partition function is computed by using measured/estimated mean numbers of baryons/anti-baryons in full phase space. In line with the experimental situation, different acceptances for baryons and anti-baryons are introduced. The results demonstrate that, overall, the experimental data follow the non-critical baseline predictions well without statistically significant differences even at the lowest energy and up to cumulant order four. Moreover, a dedicated software package with a graphical user interface is developed which allows for symbolic derivations of net-baryon cumulants of any order. The ALICE data strongly indicate long-range correlations, implying sensitivity to early stages of collisions. The presented framework can be used in the next generation of experiments at RHIC and the LHC as well as at future facilities such as NICA and GSI/FAIR.

The author acknowledges important and instructive discussions with Peter Braun-Munzinger, Bengt Friman, Krzysztof Redlich and Johanna Stachel. This work is part of and supported by the DFG Collaborative Research Centre “SFB 1225 (ISOQUANT)”.

REFERENCES

- [1] P. Braun-Munzinger, J. Wambach, *Rev. Mod. Phys.* **81**, 1031 (2009).
- [2] A. Andronic, P. Braun-Munzinger, K. Redlich, J. Stachel, *Nature* **561**, 321 (2018).
- [3] P. Braun-Munzinger *et al.*, [arXiv:2007.02463](https://arxiv.org/abs/2007.02463) [nucl-th].
- [4] Y. Aoki *et al.*, *Nature* **443**, 675 (2006).
- [5] A. Bazavov *et al.*, *Phys. Lett. B* **795**, 15 (2019).
- [6] R.D. Pisarski, F. Wilczek, *Phys. Rev. D* **29**, 338 (1984).
- [7] M. Asakawa, K. Yazaki, *Nucl. Phys. A* **504**, 668 (1989).
- [8] K. Rajagopal, F. Wilczek, *Nucl. Phys. B* **399**, 395 (1993).

- [9] A.M. Halasz *et al.*, *Phys. Rev. D* **58**, 096007 (1998).
- [10] M.A. Stephanov, K. Rajagopal, E.V. Shuryak, *Phys. Rev. Lett.* **81**, 4816 (1998).
- [11] M. Stephanov, *Phys. Rev. D* **73**, 094508 (2006).
- [12] B.-J. Schaefer, J. Wambach, *Phys. Rev. D* **75**, 085015 (2007).
- [13] C. Sasaki, B. Friman, K. Redlich, *Phys. Rev. Lett.* **99**, 232301 (2007).
- [14] H.-T. Ding, F. Karsch, S. Mukherjee, *Int. J. Mod. Phys. E* **24**, 1530007 (2015).
- [15] M. Buballa, S. Carignano, *Phys. Lett. B* **791**, 361 (2019).
- [16] V. Koch, «Hadronic Fluctuations and Correlations», in: R. Stock (Ed.) «Relativistic Heavy Ion Physics of Landolt–Börnstein — Group I ‘Elementary Particles, Nuclei and Atoms’. Vol. 23», *Springer-Verlag, Berlin Heidelberg* 2010, pp. 626–652.
- [17] L. Adamczyk *et al.*, *Phys. Rev. Lett.* **112**, 032302 (2014).
- [18] A. Rustamov, *Nucl. Phys. A* **967**, 453 (2017).
- [19] M. Arslanodok, «Recent results on net-baryon fluctuations in ALICE», in: «Proceedings of 28th International Conference on Ultrarelativistic Nucleus–Nucleus Collisions», 2020.
- [20] S. Acharya *et al.*, *Phys. Lett. B* **807**, 135564 (2020).
- [21] J. Adam *et al.*, [arXiv:2001.02852 \[nucl-ex\]](https://arxiv.org/abs/2001.02852).
- [22] M. Mackowiak-Pawlowska, «NA61/SHINE results on fluctuations and correlations at CERN SPS energies», in: «Proceedings of 28th International Conference on Ultrarelativistic Nucleus–Nucleus Collisions», 2020.
- [23] J. Adamczewski-Musch *et al.*, *Phys. Rev. C* **102**, 024914 (2020).
- [24] P. Braun-Munzinger, A. Rustamov, J. Stachel, *Nucl. Phys. A* **960**, 114 (2017).
- [25] P. Braun-Munzinger, A. Rustamov, J. Stachel, *Nucl. Phys. A* **982**, 307 (2019).
- [26] A. Bzdak, V. Koch, V. Skokov, *Phys. Rev. C* **87**, 014901 (2013).
- [27] P. Braun-Munzinger, A. Rustamov, J. Stachel, [arXiv:1907.03032 \[nucl-th\]](https://arxiv.org/abs/1907.03032).
- [28] V. Begun, M. Gazdzicki, M.I. Gorenstein, O. Zozulya, *Phys. Rev. C* **70**, 034901 (2004).
- [29] V. Vovchenko *et al.*, *Phys. Lett. B* **811**, 135868 (2020).
- [30] M. Barej, A. Bzdak, [arXiv:2006.02836 \[nucl-th\]](https://arxiv.org/abs/2006.02836).
- [31] P. Braun-Munzinger, K. Redlich, J. Stachel, [arXiv:nucl-th/0304013](https://arxiv.org/abs/nucl-th/0304013).
- [32] R. Hagedorn, K. Redlich, *Z. Phys. C* **27**, 541 (1985).
- [33] M. Gorenstein, W. Greiner, A. Rustamov, *Phys. Lett. B* **731**, 302 (2014).
- [34] A. Bazavov *et al.*, *Phys. Rev. D* **101**, 074502 (2020).
- [35] H. Appelshauser *et al.*, *Phys. Rev. Lett.* **82**, 2471 (1999).

- [36] I. Arsene *et al.*, *Phys. Lett. B* **677**, 267 (2009).
- [37] B. Friman, A. Rustamov, git clone
<https://github.com/e-by-e/Cumulants-CE.git>
- [38] M. Gaździcki, K. Grebieszko, M. Maćkowiak, S. Mrówczyński, *Phys. Rev. C* **83**, 054907 (2011).
- [39] M. Gorenstein, *Phys. Rev. C* **84**, 024902 (2011); *Erratum ibid.* **97**, 029903 (2018).
- [40] A. Rustamov, M. Gorenstein, *Phys. Rev. C* **86**, 044906 (2012).
- [41] M. Arslanok, A. Rustamov, *Nucl. Instrum. Methods Phys. Res. A* **946**, 162622 (2019).
- [42] M. Gaździcki, M. Gorenstein, M. Mackowiak-Pawłowska, A. Rustamov, *Nucl. Phys. A* **1001**, 121915 (2020).
- [43] M. Gyulassy, X.-N. Wang, *Comput. Phys. Commun.* **83**, 307 (1994).
- [44] A. Dumitru, F. Gelis, L. McLerran, R. Venugopalan, *Nucl. Phys. A* **810**, 91 (2008).